

A Comparison Of Gravity Filtering Methods Using Wavelet Transformation And Moving Average (A Study Case Of Pre And Post Eruption Of Merapi In 2010 Yogyakarta, Indonesia)

Rina D Indriana^{1*}, Kirbani S. Brotopuspito², Ari Setiawan² And Tarcisius A Sunantyo³

¹Department of Physics, Universitas Diponegoro, Semarang, Indonesia

²Department of Physics, Universitas Gadjah Mada, Yogyakarta, Indonesia

³Department of Geodetic Engineering, Universitas Gadjah Mada, Yogyakarta, Indonesia

* Corresponding Author: Rina D Indriana¹

Abstract: Merapi had a big eruption in 2010. This eruption caused a change in its mass distribution. The changes of mass distribution can be identified by the local and regional anomalies of gravity data. The separation of local and regional anomalies can be done by applied a data filtering method using wavelet transformation and moving average. The assumed data are used is a 2-period data with a separate distribution. A comparison between two methods is used to obtain a more detailed anomaly separation. The result are wavelet transformation method able to separate the local anomaly more detail than the moving average method. Anomaly value in wavelet transform method is ranging between 1.0 mGal to 2.8 mGal while moving average method is ranging between 0.2 mGal to 2.2 mGal. A higher anomaly value indicates an increase of density variation. Local anomalies that appear in the pre and post-eruption of 2010 are located to the southeast part of the Merapi's peak supposed as its reservoir and other gravity anomalies in the northwest are suspected as low-density regions.

Keywords - Merapi, Gravity data, filtering, moving average, wavelet transformation.

Date of Submission: 11-05-2018

Date of acceptance: 26-05-2018

I. Introduction

Merapi eruption in 2010 release volcanic materials approximated 150 m² causing a topographical deformation on the peak of Merapi. The number of volcanic materials resulted in the mass distribution change of Merapi. This mass distribution is also known as density variation. The change of mass distribution can be observed from the anomaly changes. Subsurface density variation is the source of gravity anomaly. The measured gravity anomaly is the amount of all anomalous subsurface sources. Gravity anomaly sources are the local and regional density variation of the underlying rocks in the research area. The difference in density between layers vertically and horizontally is referred as the density contrast. The value of this density contrast can be positive and negative.

Gravity anomalies can be seen as a superposition of multiple wavelengths in spatial domain. Each wavelength represents an anomalous source. Regional anomalies correlates with long wavelengths and local anomalies correlates with medium wavelengths. Meanwhile, noise is associated with short wavelengths. Regional anomalies have long waves in response to large and deep sources. on the other hand, local anomalies have medium waves in response to smaller and shallower sources.

For interpretational needs, local anomalies, regional anomalies and noise should be separated. The separation of local and regional anomalies can be done by using several filtering methods such as surface fitting, graphical methods with Gridding, second derivative methods, and frequency filter methods. Meanwhile, there are several available methods regarding the frequency filtering such upward, moving average, polynomial, and wavelet transform ((Argawal, 2015); (Ghuo, 2013); (Martin, 2011); (Keating, 2011); (Telford, 1999); (Blakely, 1995); (Foster et al, 1994); (Mickus, 1991)). The reductions of regional or local anomalies from Bouguer anomalies are required to extract local and regional gravitational anomalies. The common anomaly separation process practices upward continuation and moving average method. In most cases, this method is used because its simplicity. Another filtering process that has not been used to separate the anomaly is the wavelet transform method.

Wavelet-based transformation method can be practised to analyze non-stationary signals. The wavelet analysis can be used to indicate dynamic signals ((Ali, 2016); (Changbo, 2015); (Xu, 2009); (Zhang and Qiu,

1998); (Graps, 1995); (Kumar, 1994)) wavelet also used to filter and improve the data quality. Wavelet transform method commonly used for seismic analysis signals which based on time series (Zhang and Wu, 2012); (Panet, 2011); (Diao, 2009); (Li, 1997)). In gravity method, the use of wavelet decomposition method enables to separate low and high frequencies. In this research, anomaly separation process using wavelet transform and moving average method is used to compare the results of both method which of the two methods shows better detailed local anomalies. Both methods are used to generate local and regional anomalies of the Merapi volcano on the prior condition in the pre and post-eruption of 2010.

II. Method

2.1. Gravity Survey

The area of research is 25 km x 27 km wide, located in Merapi, Central Java. The gravity data is a secondary data which took in 1998 and 2011 provided by the Geophysics laboratory, Universitas Gadjah Mada. The 1998 data is the pre-eruption data consist of 248 data points and the 2001 data is the post-eruption data consist of 198 data points. Each point was repeated 3 times of measurements with each of measurement duration consist of 15 – 3 minutes. The instruments that were used in this research is a LaCoste & Romberg gravimeter type D, a single pair of Trimble GPS and other supporting hardware. The used software in this study is Surfer version 13 and Matlab. The data in this study consist of main data and supporting data. The main data are the gravity data and GPS. The gravity data is provided by the Geophysics Laboratory of Universitas Gadjah Mada. The other main data is a location data with GPS. Data processing is supported with DEM data. The DEM data within the period of 1997 to 2000 is a Sandwell DEM, which obtained from Topex period (ftp://topex.ucsd.edu/pub/srtm30_plus/) and the 2011 data using 2011 Lidar obtained from the Volcanology Agency. Measurement points distribution in 1998 and 2011 are shown in Fig.1.

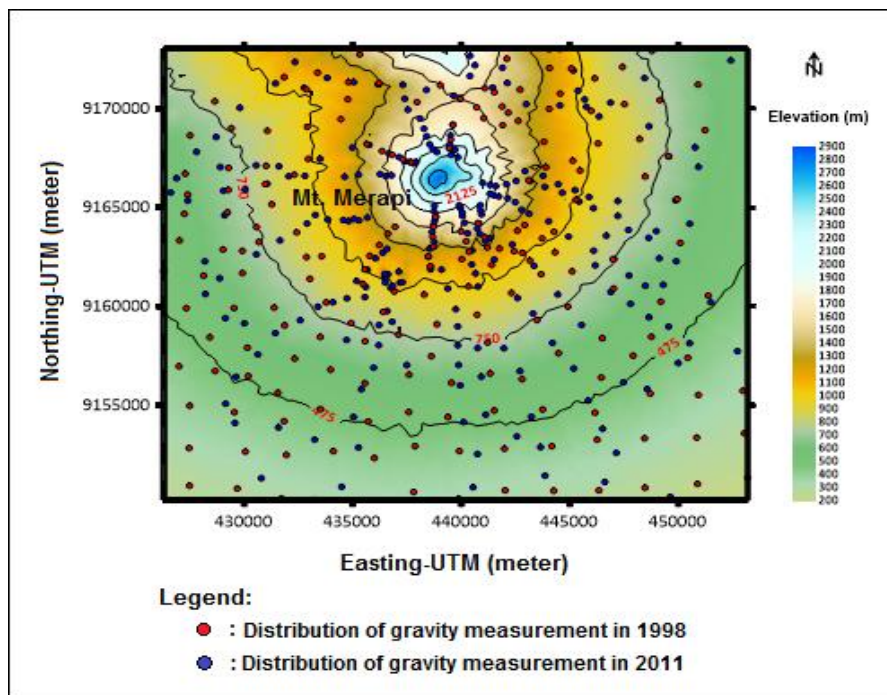


Fig.1. Distribution of gravity data measurement points 1998 and 2011 projected on UTM system; + is gravity measurement points in 2011, • is gravity measurement points in 1998.

Gravitational force is described by Newton as the attraction force between particles. This law explains that the attraction forces between two particles differentiated by the distance from their centre of mass are proportional to the magnitude of the two particles and inversely proportional to the quadratic of distance. Gravity method is known for its complete Bouguer anomaly. This complete Bouguer anomaly is the change between theoretical gravitational force and observed gravitational force. The complete Bouguer anomaly in topography is expressed as:

$$\Delta g_{BL} = g_{obs} - (g_n - FA + B - T) \tag{1}$$

Where Δg_{BL} is Complete Bouguer Anomaly (CBA), g_{obs} is observed gravity, g_n is normal gravity, FA is Free Air Anomaly, B is Bouguer Correction and Terrain Correction (Fehr, 2012). Complete Bouguer Anomaly consists of local and regional anomalies. To interpret the model we must separate regional anomalies from their local counterparts. Regional anomalies display subsurface structural model, whereas local anomalies display a shallower structural model ((Changbo, 2015); (Telford, 1999); (Blakely, 1995)). Regional and local anomalies are separated to identify the anomalies, respectively. The filtering method that is being used in this research is Wavelet transform and Moving average.

Wavelet transform is a filtering method that uses a specific function to analyze the signal variation. Wavelets and moving averages applied similar mathematical concept of FFT (Fast Fourier Transform). Moving Average used to find window size $n \times m$ and Wavelet Transform applied the mother wavelet for its FFT process.

2.2. Moving Average Method

The Moving Average method can be used to distinguish regional and local anomalies/residuals using similar concept with low-pass filters. The Moving Average method allows the low-frequency signal from Bouguer anomalies to pass, and the result are regional anomaly. Then the residual anomaly were obtained by subtracting the total Bouguer anomaly from the regional anomalies. Mathematically expressed as follows.

$$\Delta g_{(i,j)} = \Delta g_{reg(i,j)} + \Delta g_{res(i,j)} \tag{2}$$

$$\Delta g_{reg\left(\frac{n+1}{2}, \frac{m+1}{2}\right)} = \sum_{i=1}^n \sum_{j=1}^m \frac{\Delta g_{(i,j)}}{\left(\frac{n+m}{2}\right)} \tag{3}$$

and its corresponding residual anomaly is given by:

$$\Delta g_{res(i,j)} = \Delta g_{(i,j)} - \left[\sum_{i=1}^n \sum_{j=1}^m \frac{\Delta g_{(i,j)}}{\frac{n+m}{2}} \right] \tag{4}$$

$\Delta g_{(reg(i,j))}$ is the regional anomaly in row I and column j, $\Delta g_{res(i,j)}$ is the residual anomaly on row I and column j, $\Delta g_{((i,j))}$ is the complete Bouguer anomaly row I and column j, n is the window size, and m is the window size (Blakely, 1995).

Determining the value of $n \times m$ can be done by using spectrum analysis. Spectrum analysis usually used to determine the depth boundary layer. This spectrum analysis is done by running FFT process. By using FFT we able to calculate the value of wavenumber (k) and amplitude (A). The wavenumber and amplitude will be used in the calculation of the window size in the screening process of the moving average method. The relationship between amplitude (A) with wavenumber (k) and depth ($Z_0 - Z$) can be obtained by its amplitude spectral logarithm. The amplitude of spectral logarithm produce a linear equation where k is directly proportional to A:

$$\ln A = (z_0 - z')|k| + \ln C \tag{5}$$

The amplitude spectrum logarithm is a linear equation. The depth of regional, residual, and noise anomalies are known from their trend line gradients. The gradient graph is a plotted line on a spectral amplitude log graph. The trend line intersection between regional and residual zone boundaries is used to calculate the filter window size (n and m) on Moving Average method. The equations are:

$$n = \frac{2\pi}{k\Delta x} \tag{6}$$

Which k is wave number and Δx is space grid of data. A number of n and m used to be window size in the moving average process.

2.3. Wavelet Transform

Fourier transforms theory states that signals can be expressed as a limited number of sine and cosine series. This number is known as the Fourier series (or Fourier expansion). Fourier series only have frequency resolution with no time resolution. The Fourier transformation is able to display the entire present frequencies in a signal form but it is largely unknown when will the signal occurs. So, Wavelet transform is used to solve this problem. Wavelet is a mathematical function that divides data into several different frequency components and analyzes each of these components by using the appropriate scale resolution. Wavelet transform has the advantage as compared with Fourier transform in terms of signal analysis ability to analyze non-stationary signals. ((Graps, 1995); (Yang et al, 2001); (Diao, 2009)).

The Wavelet theory was first introduced by Haar in 1904 known as the Haar Wavelet (Zhang et al, 1998). The Wavelet concept then developed by Morlet and Grossman in 1984 with an orthogonal wavelet which was later developed by Meyer. Mallat and Meyer proposed the concept of multi-resolution and the support of compact orthogonal wavelet by Daubechies (Zhang et al, 1998). Wavelet is a function of the real x variable, denoted as the parent wavelet. The expressed wavelet equation as follows:

$$\int_{-\infty}^{\infty} \psi(t) dt = 0 \tag{7}$$

Suppose the scaling function and wavelet function are the basis, a discrete signal in $L_2(Z)$ can be approximated as:

$$F[n] = \frac{1}{\sqrt{M}} \sum_k W_{\phi}[j_0, k] \phi_{j_0, k}[n] + \frac{1}{\sqrt{M}} \sum_{j=j_0}^{\infty} \sum_k W_{\psi}[j, k] \psi_{j, k}[n] \tag{8}$$

$F[n]$, $\phi_{j_0, k}[n]$ and $\psi_{j, k}[n]$ is a discrete function in $[0, M - 1]$ with M total point, $\psi_{j, k}[n]$ is translation equation of wavelet, $\phi_{j_0, k}[n]$ is dilatation equation of wavelet, j is dilatation parameter, k is translation parameter, n is integer, Z is time series (Liu, 2010). Because of $\{\phi_{j_0, k}[n]\}_{k \in Z}$ and $\{\psi_{j, k}[n]\}_{(j, k) \in Z^2, j \geq j_0}$ is orthogonal each other, wavelet Coefficient can be defined as:

$$W_{\phi}[j_0, k] = \frac{1}{\sqrt{M}} \sum_n f[n] \phi_{j_0, k}[n] \tag{9}$$

$$W_{\psi}[j, k] = \frac{1}{\sqrt{M}} \sum_n f[n] \psi_{j, k}[n] \quad j \geq j_0 \tag{10}$$

$W_{\phi}[j_0, k]$ is approximation coefficient and $W_{\psi}[j, k]$ is coefficient detail. Another formula can be used to find the wavelet coefficient when translation and dilatation of wavelet function is unknown. We can construct dilatation and translating as a basis form of wavelet function into dilatation and translation equation with reduce the computation time (Liu, 2010).

$$\psi_{j_0, k}[n] = 2^{j/2} \psi[2^j n - k] \tag{11}$$

$$\phi_{j_0, k}[n] = 2^{j/2} \phi[2^j n - k] \tag{12}$$

Coefficient approximation equation become:

$$W_{\phi}[j, k] = \frac{1}{\sqrt{M}} \sum_n f[n] \phi_{j, k}[n] \tag{13}$$

$$= h_{\phi}[-n] * W_{\phi}[j + 1, n] |_{n=2k, k \geq 0} \tag{14}$$

With same step we can find coefficient detail is:

$$W_{\psi}[j, k] = h_{\psi}[-n] * W_{\phi}[j + 1, n] |_{n=2k, k \geq 0} \tag{15}$$

Next level approximation and detail can be obtain by using equation 14 and 15. This equation more simple to find the coefficients every level. In the 2D wavelet transform, the dilatation and translation function become two variable function $\phi(x, y)$ and $\psi(x, y)$ (Liu 2010). the function define as:

$$\phi_{j, m, n}(x, y) = 2^{j/2} \phi(2^j x - m, 2^j y - n), \tag{16}$$

$$\psi_{j, m, n}(x, y) = 2^{j/2} \psi(2^j x - m, 2^j y - n), \quad i = \{H, V, D\} \tag{17}$$

Than 2D discrete wavelet transform of coefficient approximation and coefficient detail are (Liu, 2010):

$$W_{\phi}(j_0, m, n) = \frac{1}{\sqrt{MN}} \sum_{x=0}^{M-1} \sum_{y=0}^{N-1} f(x, y) \phi_{j_0, m, n}(x, y) \tag{18}$$

$$W_{\psi}^i(j, m, n) = \frac{1}{\sqrt{MN}} \sum_{x=0}^{M-1} \sum_{y=0}^{N-1} f(x, y) \psi_{j, m, n}^i(x, y), \quad i = \{H, V, D\} \tag{19}$$

$$f(x, y) = \frac{1}{\sqrt{MN}} \sum_m \sum_n W_{\phi}(j_0, m, n) \phi_{j_0, m, n}(x, y) + \frac{1}{\sqrt{MN}} \sum_{i=H, V, D} \sum_{j=j_0}^{\infty} \sum_m \sum_n W_{\psi}^i(j, m, n) \psi_{j, m, n}^i(x, y) \tag{20}$$

Wavelet transforms known with several algorithms such Continuous Wavelet Transforms (CWT) and Discrete Wavelet Transforms (DWT). DWT is more simple than CWT. DWT is a wavelet decomposition process that able to divide each input accordingly as same as the parent wavelet. The first phase of

decomposition process is to determine the low and high-frequency values of an input. The frequency determination process is to input a certain low pass filter (LPF) signal to obtain a high-frequency value and then the prior signal surpasses through a high pass filter (HPF) to obtain the low-frequency value. Then the downsampling process occurs on two-part output. The value of LPF and HPF depends on the type of wavelet being used.

Each step of wavelet transform calculates the average values and the sets of wavelet coefficient. If there were datasets of $S_0, S_1, S_2, \dots, S_{N-1}$, each data contains wavelet elements then there will be $N/2$ mean value and $N/2$ coefficient value. The average value sets are kept $1/2$ less than of N value and the coefficient value sets are kept $1/2$ more than N . The average value sets will be the next input of the calculation process. The stages of wavelet processing using programming as follows: create data input, select the type of wavelet transformation method, specify the parent wavelet and the programming instructions.

III. Result

The results of gravity data processing in 2011 as follows:

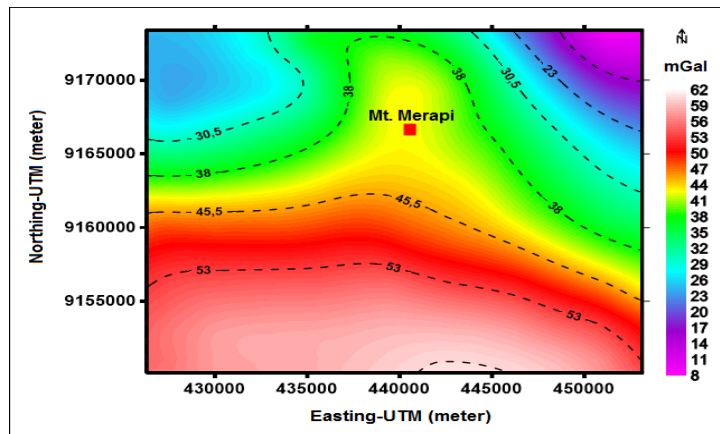


Fig.2. Gravity anomaly on Flat Plane of Merapi in 2011 projected on UTM system

The value of 2011 gravity anomaly on a flat plane is between 8 to 64 mGal. High anomaly values present in the Southern part of Merapi and decrease to the North.

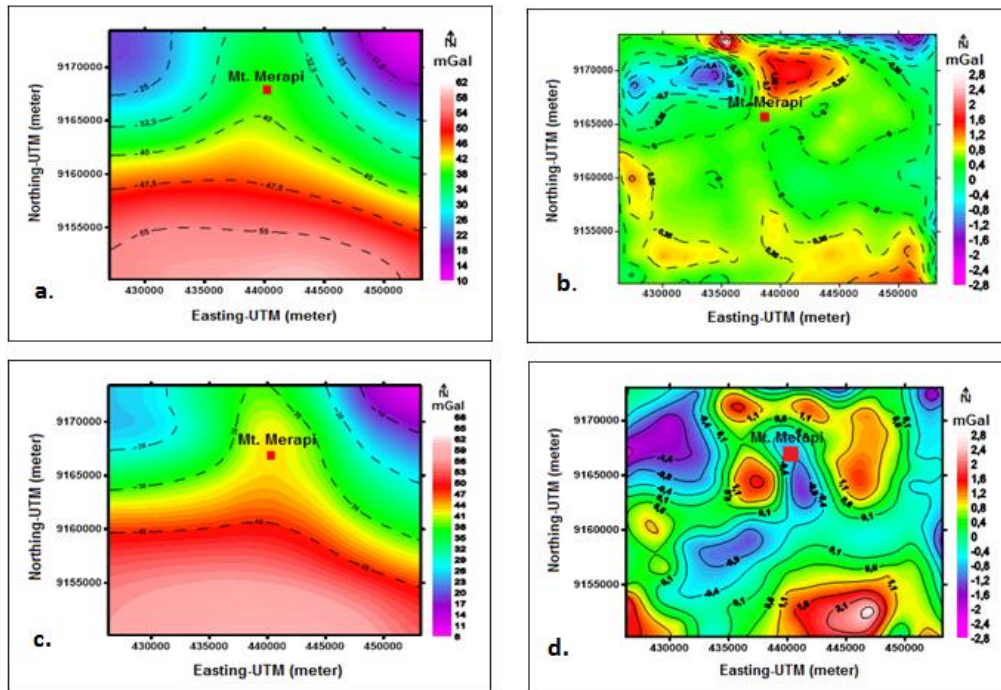


Fig.3. Results of local and regional anomalies filtering of 2011 gravity data projected on UTM system; a. Regional anomaly from moving average filtering, b. Local anomaly from moving average filtering, c. Regional anomaly from wavelet filtering, and d. Local anomaly from wavelet filtering.

The filtering process of Merapi gravity data utilizing Wavelet transform and Moving average method are shown in Fig.3. The gravity data that are being used are from 2 separate group of datasets in the same area of research. (2 epoch: 1998 and 2011). The results showed that filtering process using Wavelet transform and Moving average method had the similar values between 8 to 64 mGal for regional anomalies, and -2.8 to 2.8 mGal for local anomalies (Fig.3.)

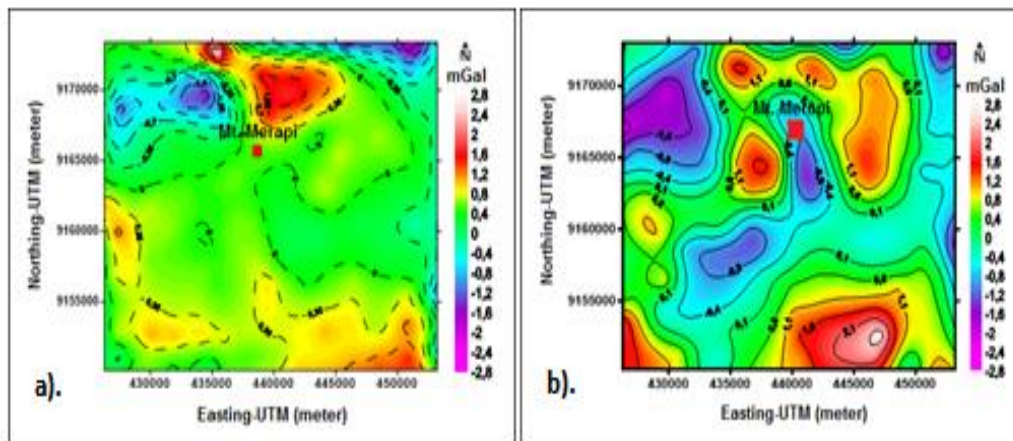


Fig.4. Results of local anomalies processing of 2011 gravity data projected on UTM system; a. Local anomaly from moving average, b. Local anomaly from wavelet transform, ■ is Merapi’s peak.

Wavelet transform and Moving average method showed a similar trend (Fig.4). Wavelet transform method could achieve a detailed contour of local anomalies compared with Moving average method on the same datasets on 2011 (Fig.5).

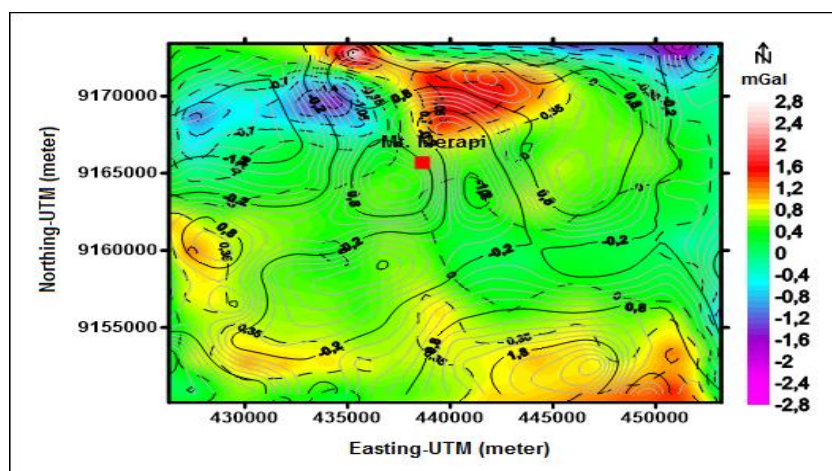


Fig.5. Local anomaly gravity data 2011 by moving averages filtering that is overlain with local anomaly by wavelet filtering, projected on UTM system. Colour contour for moving average filtering and Line contour for wavelet filtering, ■ is Merapi’s peak.

Table 1. Closure distribution and Δ value of closure (local anomaly data in 2011)

Gravity Anomaly data 2011	Moving average Value (mGal)	Wavelet transform Value (mGal)
North	0.2 – 2.2	0.0 – 1.6
North-East	-1.8 – 0.2	-1.6 – 0.8
North-West	-1.8 – 0.2	-2.0 – 0.0
West	0.0 – 0.2	0.2 – 1.0
East	-0.4 – 0.2	-1.2 – (-0.2)
South	0.2 – 0.6	0.2 – 1.4
South-east	0.2 – 0.6	0.2 – 2.8
South-west	0.2 – 0.8	0.2 – 1.4
Around summit	-1.0 – 0.4	-1.2 – 1.6

Table 2. Closure distribution of Moving Average and Wavelet Transform (local anomaly data in 2011)

Gravity Anomaly data 2011	Moving average closure	Wavelet transform closure
North	Y	Y
North-East	Y	Y
North-West	Y	Y
West	N	Y
East	N	Y
South	N	N
South-east	N	Y
South-west	N	Y
Around summit	Y	Y

Table 3. Δ value of Moving Average and Wavelet Transform (local anomaly data in 2011)

Gravity anomaly data 1998	Moving average	Wavelet transform
	Δ Value (mGal)	Δ Value (mGal)
North	1.2	1.6
North-East	2.0	2.4
North-West	2.0	2.0
West	0.2	0.8
East	0.6	1.0
South	0.4	1.2
South-east	0.4	2.6
South-west	0.4	1.2
Around summit	1.4	2.8

The result of local anomalies of gravity data in 2011 expressed that Moving average shows the values between -1.8 to 2.2 mGal, whereas Wavelet transforms between -1.6 to 2.6 mGal (Table 1). The Δ value of Moving average is between 0.2 to 2.2 and 0.8 to 2.8 mGal is for Wavelet Transform (Table 3). Results of 1998 gravity data processing on flat plane (Fig... 6) are as follow:

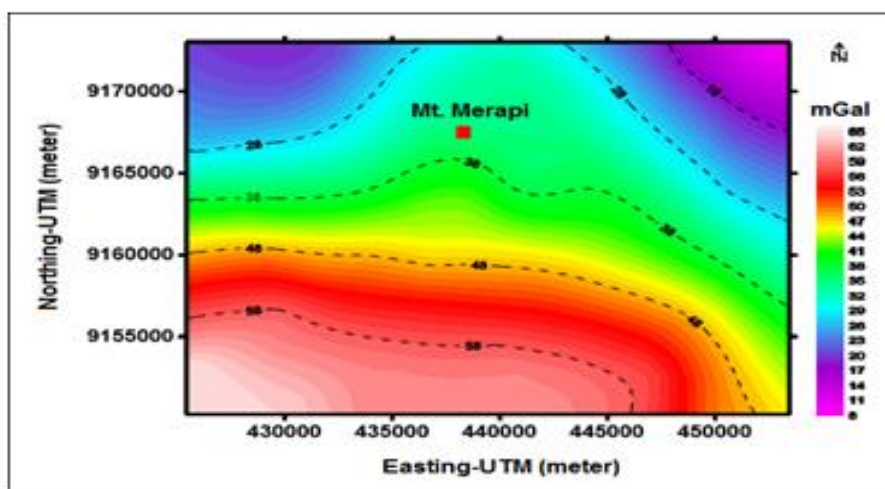


Fig.6. Gravity anomaly on Flat Plane (3000 m) of Merapi in 1998, projected on UTM system, ■ is Merapi's peak

The value of gravity anomaly in 1998 was a positive value ranging between 8 to 64 mGal. The high anomalies identified located on the South and decrease to the North.

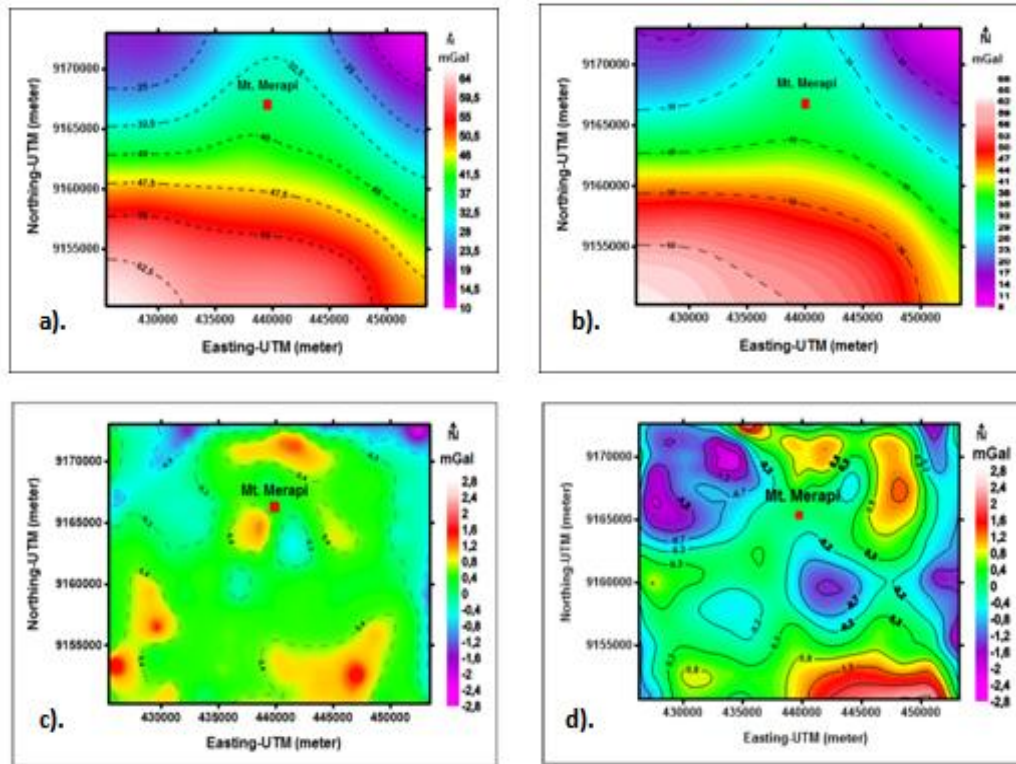


Fig.7. Results of local and regional anomalies processing of 1998 gravity data, projected on UTM system; a. Regional anomaly from moving average filtering. b. Local anomaly from moving average filtering. c. Regional anomaly from wavelet filtering. d. Local anomaly from wavelet filtering, ■ is Merapi's peak. The results of Wavelet transform and Moving average method on the gravity data in 1998 shown similar values between 8 to 64 mGal for regional anomalies, and -2.8 to 2.8 mGal for local anomalies.

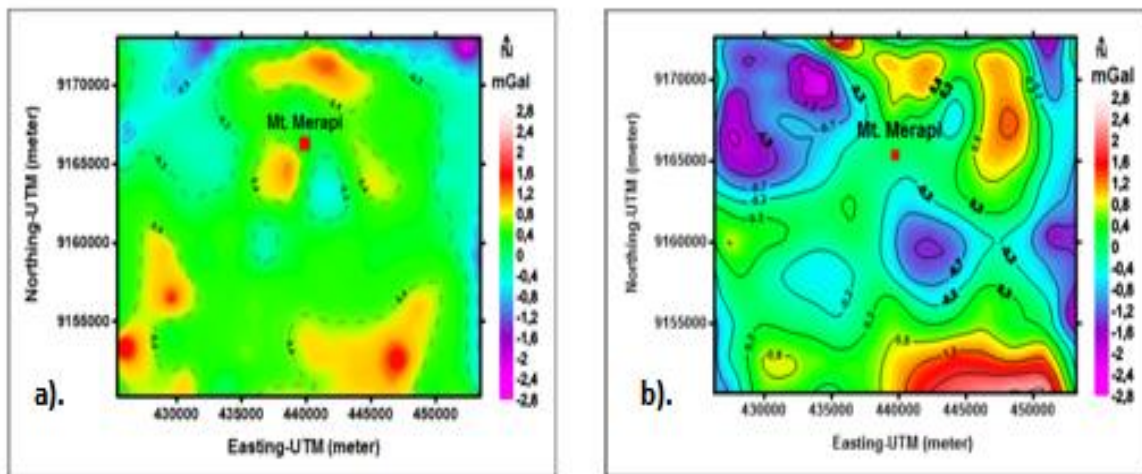


Fig.8. Results local and regional anomalies processing of 1998 gravity data, projected on UTM system; a. Local anomaly from wavelet filtering. b. Local anomaly from moving average filtering, ■ is Merapi's peak. Wavelet transform and Moving average method showed a similar trend (Fig.9). Wavelet transformation could achieve a detailed contour of local anomalies compared with Moving average method on the same datasets on 1998 (Fig.8).

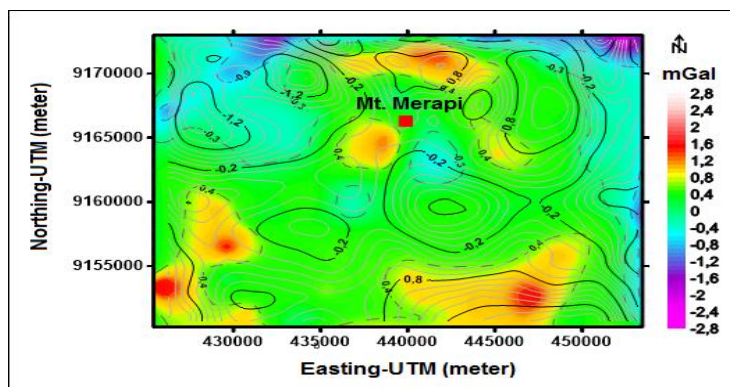


Fig.9. Local anomaly from moving average filtering that is overlain with local anomaly from wavelet filtering gravity data 1998, projected on UTM system. Colour contour for moving average method, Line contour for wavelet method and ■ is Merapi’s peak

The result of local anomalies of gravity data in 1998 expressed that Moving average shows the values between -1.2 to 1.0 mGal, whereas Wavelet transforms between -1.2 to 2.6 mGal. The Δ value of Moving average is between 0.2 to 2.2 and 0.8 to 2.8 mGal is for Wavelet Transform (Table 4, 6).

Table 4. Local anomaly of gravity data 1998 by using Moving Average and Wavelet Transform

Gravity anomaly data 1998	Moving average	Wavelet transform
	Value (mGal)	Value (mGal)
North	0.0 – 0.8	0.2 – 1.2
North-East	-1.2 – 1.0	0.8 – 0.8
North-West	-1.2 – 0.2	-2.0 – 0.2
West	-0.2 – 0.2	0.2 – 1.0
East	-0.8 – (-0.2)	-1.2 – (-0.2)

Table 5. Closure distribution of Moving Average and Wavelet Transform (local anomaly data in 1998)

Gravity anomaly data 1998	Moving average closure	Wavelet transform closure
North	Y	Y
North-East	Y	Y
North-West	Y	Y
West	N	Y
East	N	Y
South	N	N
South-east	Y	Y
South-west	N	Y
Around summit	Y	Y

Table 6. Δ value of Moving Average and Wavelet Transform (local anomaly data in 1998)

Gravity anomaly data 1998	Moving average	Wavelet transform
	Δ Value (mGal)	Δ Value (mGal)
North	0.8	1.0
North-East	2.2	1.6
North-West	1.4	2.2
West	0.4	0.8
East	0.6	1.0
South	0.2	0.6
South-east	0.8	2.4
South-west	0.6	1.4
Around summit	2.0	2.8

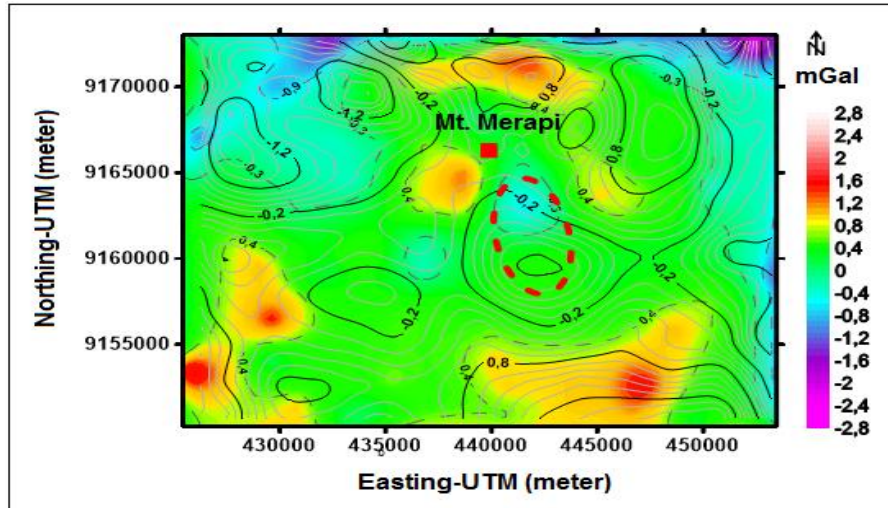


Fig.10. Strike pattern of reservoir position obtained from 1998 gravity data, projected on UTM system. Colour contour for moving average filtering and Line contour for wavelet filtering, ■ is Merapi's peak and - - - is anomalous area which predicted as reservoir.

Overlay process between this two methods for gravity data in 1998 shows 2 areas of anomaly. North-West and South-East side of Merapi's peak. The anomaly value ranging between -2.2 mGal to -0.4 mGal. Red dotted-line is the predicted area of the reservoir. (Fig.10).

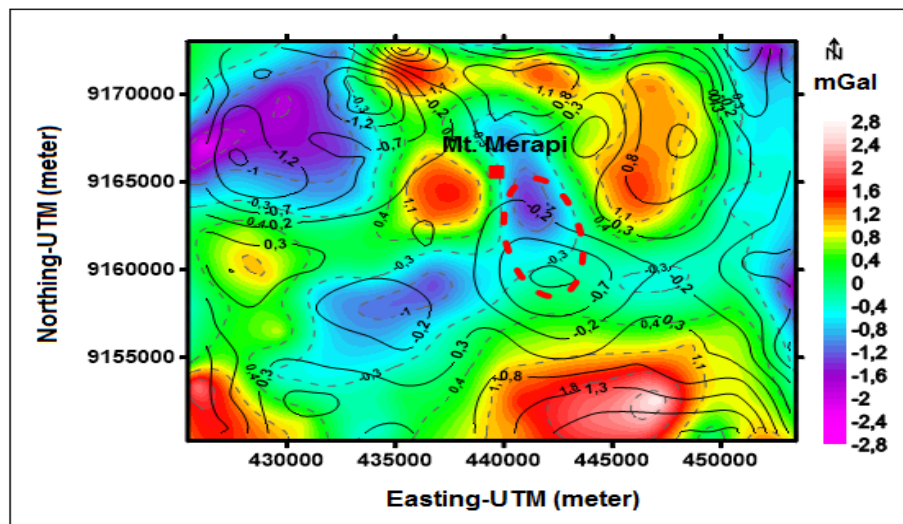


Fig.11. Local anomaly in 1998 that is overlain with local anomaly in 2011, projected on UTM system. Colour contour for wavelet filtering data 1998, line contour for wavelet filtering data 2011, ■ is Merapi's peak and - - - is anomalous area which predicted as reservoir.

The overlain data between 2 epochs of gravity data using Wavelet transform method shows two areas of anomaly on the North-West and South-East side of Merapi's peak. The anomaly value ranging between -2.2 mGal to -0.4 mGal. The red dotted-lines are the predicted area of the reservoir (Fig.11).

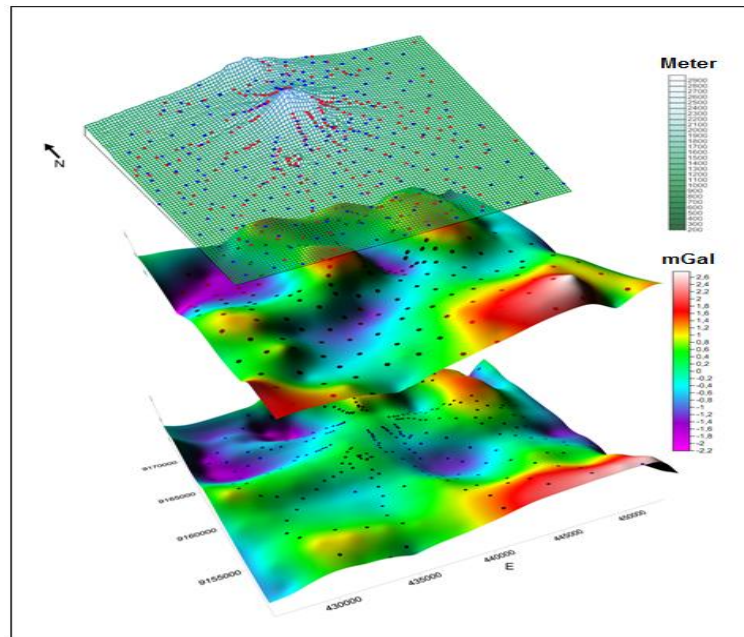


Fig.12. Local anomaly in 1998 that is overlain with local anomaly in 2011 and topographic, projected on UTM system. Colour contour for wavelet filtering data 1998 and 2011, line contour for topographic surface, ● is gravity station in 2011 and ● is gravity station in 1998.

The wavelet results overlain with topographic show consistent anomaly pattern on northwest, southwest and southeast. Pattern changing show at southeast area, there is on Merapi reservoir area (**Fig.12**)

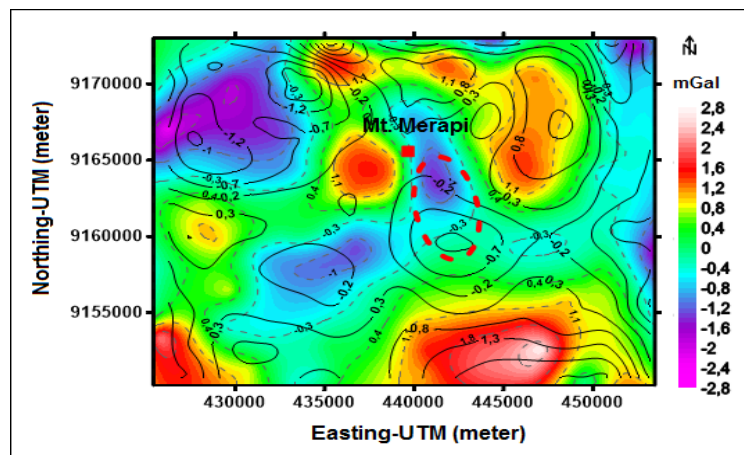


Fig.13. Local anomaly in 2011 that is overlain with local anomaly in 1998 (moving average filtering), projected on UTM system. Colour contour for moving average filtering data 2011, Line contour for moving average filtering data 1998 and ■ is Merapi's peak

Overlain process between both two epoch gravity data which use wavelet method, show 2 anomalous area. Interesting area show on northwest, southwest and southeast of Merapi peak. Anomalous values are -2.2 mGal to -0.4 mGal. The red dash line is an area which predicted as reservoir (**Fig.11**).

IV. Discussion

The complete Bouguer anomaly contour map which consists of 2 gravity data sets with same area in 2 epochs (1998 and 2011) are shown in **Fig.2** and 6. The gravity data filtering of Merapi using Wavelet transform and Moving average method shown in **Fig.3** and 7. Local and regional anomalies show a layer of density variation and subsurface model. Local anomalies have more variety of contour compared to the regional anomaly. Regional anomaly contours did not show a significant difference between Wavelet transform and Moving average method filtering. Both methods expressed the similar data trends. The distinct difference is shown on the local anomaly contour trends (**Fig.3** and 7). Local anomaly produce a more detailed contour by utilizing the Wavelet transform method, compared with Moving average method. Nevertheless, both methods

show a similar contour trend (**Fig.4** and **8**). Local anomaly shows the presence of varied local layering. Both expressed similar trends with a slight difference in the anomaly areas. Therefore, both of Wavelet transform and Moving average method could result in similar trend pattern, but Wavelet transform results are more detailed (**Fig.5** and **9**).

The value of Wavelet transform and Moving average method for gravity data in 2011 are between 8 to 64 mGal for regional anomalies, and -2.8 to 2.8 mGal for local anomalies (**Fig.3**). The moving average method shows the value between -0.2 to 0.4 mGal on the Southern and South-East part of Merapi's peak. The value on the North peak is between 0.8 to 2 mGal, whereas on North-West and South-West ranging between -0.8 to -2.8. This method shows a closure on the peak that indicates the appearance of the reservoir are not present. Meanwhile, the wavelet method resulted between -0.4 to -2.8 mGal on the South, North, and West side of the peak. This method is also capable to show a closure pattern near the peak, especially on the South-East and North-West side of the research area (**Fig.4**) (**Table 1**). Therefore, both of Wavelet transform and Moving average method could result in similar trend pattern, but Wavelet transform results are more detailed (**Fig. 5**). If the study area is grouped into 9 areas to observe the closure contour or not, the following results are obtained: utilizing Moving average on 5 particular areas with no closure, while only 1 area with Wavelet transform with no closure pattern (**Table 1**). The Δ value wavelet is between 1.0 to 2.8 mGal, while Δ value moving average between 0.2 to 2.0 mGal. The closure contour is not visible in the East, West, South, and South-East and South-West regions by utilizing the Moving average, but contrary with Wavelet transform method shown with closed contours. Wavelet transform is capable to produce a higher range of value. The smoothing effect of Moving average causing to produce a smaller value. The increase of Δ value indicates the complete density variety. The Wavelet transform concept is a wave decomposition that separates the signal from the compiler of a wave in detail. The Δ value can show more density variations from anomalous source or subsurface structures.

The result of the gravity anomaly filtering in 1998 utilizing Wavelet transform and Moving average method is valued between 8 to 64 mGal for regional anomaly and -2.8 to 2.8 mGal for local anomalies. The average value of local anomaly use Moving average method is -0.2 mGal to 0.8 mGal South-East, 0.2 to 1.2 mGal to the North and 0.2 to 1.2 mGal to the South side of the peak. In the West side valued between -0.8 to -2.8 mGal and -0.8 to -2.0 mGal to the East. While the Wavelet transforms method result at between -0.4 to -1.2 mGal around the peak, and -0.4 to -2.8 mGal from North-East to East. The anomalous values in the South and North are ranging between 0.8 to 2.8 mGal (**Fig.8**). Wavelet transform and Moving average method produce the similar pattern, with a better detail and better results with Wavelet transform (**Fig.9**).

The regional anomalies value on both methods is similar. Shown on a slight contour on the peak of Merapi. **Table 5** explains that most areas do not indicate a closure pattern when utilizing Moving average method. The results of Moving average method 4 out of 9 areas do not show a closure pattern whereas Wavelet transform method only shows 1 areas with no closure pattern. The Δ value of Wavelet transform method ranging between 1.0 to 2.8 mGal, while the Moving Average method with an average value of between 0.2 to 2.2 mGal (**Table 6**). The closure is not visible on the East, West, South and South-West areas with Moving average method, but contrary visible with Wavelet transform method. Wavelet transform method result a higher value than Moving average method caused by the smoothing effect of Moving average calculation. Interesting object is shown in the South where no closure present by these two methods.

The closure pattern in the South is unlikely appears caused by dominant anomalies on the South-East and South-West and there may no significant anomalies in the South. In the peak of Merapi, the closure pattern become more common with Wavelet transform method, although both methods tends to be similar, the appearance is better clearly by using the Wavelet transform method (**Fig.9**). The local anomalies result using Wavelet transform and Moving average method had a difference in 1998 data on the presence of closure patterns around the Merapi's peak. This closure pattern is so called as an anomaly. The presence anomaly can be predicted as the reservoirs. Both of reservoirs are located on the same alignment. The Wavelet transform method result a closure pattern located about 2 km to the South-East closure pattern result by the Moving average method. The closure pattern based on Moving average method lies beneath 2 km from the peak. The reservoir location is predicted lies 4 km with Wavelet transform method (**Fig.9**). These findings are consistent with the prior research which state the Merapi's reservoir is located on the South-East of the volcano with a depth of 2 – 3 km from the peak.

Further analysis from the Wavelet transform method for local anomalous data in 1998 and 2011. The overlain results show the change of reservoir position between 1998 and 2011. Based on 1998 data the reservoir was positioned further to the South-East as a reference to 2011, the position consists the same alignment which is the South-East side of the Merapi's peak. The local anomaly value at 2 epoch observations was between -2.2 to 0.4 mGal. This change in value may caused the subsurface density changes. The gravity value in 2011 is slightly higher than in 1998. This changes may be interpreted as magma intrusion processes and other events such as reducing process of low density/pyroclastic content in the reservoir.

Meanwhile, further analysis of Moving average method for local anomaly data in 2011 did not show as a closure as in 1998 (**Fig.14**). The different results may due to a large amount of data used for processing. The gravity data in 1998 consisted of 249 data while in 2011 consisted of 198 data. More data acquired in 1998 causing more value based on data samples used by the Moving average method and vice-versa in 2011 with a lack of data window. Moving average requires a large amount of data. Large data is beneficial in Moving average method due to data based process in $n \times m$ window. Gravity data in 1998 consist more data around the peak rather than the 2011 gravity data. The fewer data amount allows the closure to disappear on around the peak. If we have a lack of data, Wavelet transformation method is likely suggested than Moving average method.

In general, there is a tendency of a consistent anomaly patterns shown in the study area using both of filtering methods. Anomaly differentiation results show the anomalies in the South-Eastern peak of Merapi and to the North-West. Anomalies in the South-east of the peak are thought to be the reservoir of Merapi, while the North-West is considered as a low density area. According to Muller (2004) the Western part of Merapi is suspected as areas with low resistivity (1Ω) starting at depth of 300 m. The low resistivity zone can be analyzed as a conductive zone. Low conductivity materials are generally low density materials. Further research by other methods is required to support the identification of low density material in the North-West region of the research area. It is possible that low density material can be related to the Merapi's geological changes in the future.

V. Conclusion

The results of this study indicate that the Wavelet transform method has much better results for gravity data filtering rather than the Moving average method. This has proven to be a better Wavelet transform method produce local anomaly patterns rather than Moving average method. The Wavelet transform method describes data signal better than the Moving average method. The amount of data used in Wavelet transform method should be considered as it will affect the decomposition results.

Local anomalies around the peak are shown more detailed using the Wavelet transform method. The Δ value with Wavelet transform method ranging between 1.0 to 2.8 mGal, whereas Δ value Moving average method ranging between 0.2 to 2.2 mGal. The change of Δ value with the Wavelet transform method is higher than the Moving average method. The higher values may indicate the presence of more detailed density variations. Detailed values may result in more varied or detailed anomalous sources. The anomalies appeared on the South-East and North-West of part of the research area. The predicted anomalies as the Merapi's reservoir located on the South-East lies 2 – 4 km beneath the peak and other anomalies on the North-West suspected as a low-density anomaly. Further research should be conducted on the North-West side to identify the low-density material beneath the surface and also to analyze their correlation with their conductivity properties.

Acknowledgements

The authors would like to thank the Ministry of Research, Technology and Higher Education of the Republic of Indonesia for the support of funding in national strategic research fund DP2M in 2011-2012 with the chief researcher Prof. Dr. Kirbani, the authors also thank to the Geophysics Laboratory Universitas Gadjah Mada which has provided gravity data and gps data, as well as a Volcanology Agency that provides Lidar data. The author would like to thank to Geophysics Laboratory Universitas Diponegoro who helped in this research.

References

- [1] Agarwal B.N.P., S. S. (2010). A FORTRAN program to implement the method of finite elements to compute regional and residual anomalies from gravity data. *Computers & Geosciences*, 848-852.
- [2] Ali M. Al-Rahim. (2016). Separating the gravity field of Iraq by using bidimensional empirical mode decomposition technique. *Arabian Journal of Geosciences* 9, 1.
- [3] Blakely, J. R. (1995). *Potential Theory in Gravity and Magnetic Applications*. Cambridge: Cambridge University Press.
- [4] Changbo Li, L. W. (2015). Interpretations of gravity and magnetic anomalies in the Songliao Basin with Wavelet Multi-scale Decomposition. *Frontiers of Earth Science* 9:3, 427-436.
- [5] Diao B, Wang J L, Cheng X. Y. (2009). Fracture analysis based on continuous complex wavelet transform for gravity anomalies. *Geophysical Prospecting for Petroleum*, 303-306.
- [6] Fehr, L. (2012). *Fundamental of Gravity Exploration*. Geophysical Monogram Series.
- [7] Foster. D.J., Mosher. C.C. and Hassanzadeh. S. (1994). Wavelet Transform Methods for Geophysical Applications. *Soc. Expl. Geophys.*, 1465 – 1468.
- [8] Ghuo, L. M. (2013). Preferential Filtering for Gravity Anomaly Separation. *Computer & Geosciences*, 247- 254.
- [9] Graps. A. (1995). *An Introduction to Wavelets*. Loas Alamitos – CA: IEEE Computer Society.
- [10] Keating, P., & Pinet, N. (2011). Use of non-linear filtering for the regional-residual separation of potential field data. *Journal of Applied Geophysics, Volume 73, Issue 4*, 315-322.
- [11] Kumar. P. and Foufloula-Georgiou. E.. (1994). *Wavelet Analysis in Geophysics: An Introduction Wavelet in Geophysics*. USA: Academic Press Inc.
- [12] Li Z J, Yang L, Wang Q. C. (1997). Application of the wavelet transform in potential field data processing. *Geophysical Prospecting for Petroleum*, 36 (2), 86-93.
- [13] Lin, L. C. (2010). A tutorial of Wavelet Transform.

- [14] Martín, A., Núñez, M. A., Gili, J. A., & Anquela, A. B. (2011). A comparison of robust polynomial fitting, global geopotential model and spectral analysis for regional-residual gravity field separation in the Doñana National Park (Spain). *Journal of Applied Geophysics Volume 75, Issue 2*, 327-337.
- [15] Martínez-Moreno F.J., G.-Z. J.-C. (2015). Regional and residual anomaly separation in microgravity maps for cave detection: The case study of Gruta de las Maravillas (SW Spain). *Journal of Applied Geophysics 114*, 1-11.
- [16] Mickus K. L., A. C. (1991). Regional-residual gravity anomaly separation using the minimum-curvature technique. *Geophysics, 56(2)*, 279-283.
- [17] Müller A. Haak. V. (2004). 3-D modeling of the deep electrical conductivity of Merapi volcano (Central Java): integrating magnetotellurics. induction vectors and the effects of steep topography. *J Volcanol Geotherm Res 138*, 205–222.
- [18] Panet, I., Kuroishi, Y., & Holschneider, M. (2011). Wavelet modelling of the gravity field by domain decomposition methods: an example over Japan. *Geophysical Journal International, Volume 184*, 203-219.
- [19] Retnowati. E.. (2006). Metode Filtering Data Gayaberat untuk Identifikasi Cekungan Hidrokarbon di Pulau Jawa, Undergrad. Thesis, Geophysical Engineering Department. Bandung: Faculty of Earth Science and Mineral Technology, Institut Teknologi Bandung.
- [20] Sailhac P. & Gilbert. D. (2003). Identification of Sources of Potential Fields with the Continuous Wavelet Transform: Two-Dimensional Wavelet and Multipolar Approximations. *J. Geophys. Res., 108(B5)*, 2262.
- [21] Setiawan. A. (2002). Modeling of Gravity Changes on Merapi Volcano: Observed between 1997–2000, Thesis,. Darmstadt: Technischen Universität Darmstadt.
- [22] Telford, W. G. (2004). *Applied Geophysics, 2nd Edition*,. Cambridge: Cambridge University Press.
- [23] Topex. (2010). *The DEM data within the period of 1997 to 2000 is a Sandwell DEM*. Diambil kembali dari Topex: ftp://topex.ucsd.edu/pub/srtm30_plus/
- [24] Xu, Y. H. (2009). Regional Gravity Anomaly Separation Using Wavelet Transform and Spectrum Analysis. *Journal of Geophysics and Engineering*, 3.
- [25] Yang, W. S. (2001). Discrete Wavelet Transform for Multiple Decomposition of Gravity Anomalies. *J. Geophys, 44(4)*, 529-537.
- [26] Zhang C Y, Qiu Q X. (1998). Wavelet analysis and the prospects for its applications on gravity. *Progress in Geophysics* , 13 (2), 73-85.

IOSR Journal of Applied Geology and Geophysics (IOSR-JAGG) is UGC approved Journal with Sl. No. 5021, Journal no. 49115.

Rina D Indriana "A Comparison Of Gravity Filtering Methods Using Wavelet Transformation And Moving Average (A Study Case Of Pre And Post Eruption Of Merapi In 2010 Yogyakarta, Indonesia) ." IOSR Journal of Applied Geology and Geophysics (IOSR-JAGG) 6.3 (2018): 44-57